A simple model of pathogen-immune dynamics including specific and non-specific immunity

Andrea Pugliese [1,*],

Department of Mathematics, University of Trento, Trento, 38050 Italy

Alberto Gandolfi

Istituto di Analisi dei Sistemi ed Informatica del CNR, Rome, Italy

Abstract

We present and analyze a model for the dynamics of the interactions between a pathogen and its host's immune response. The model consists of two differential equations, one for pathogen load, the other one for an index of specific immunity. Differently from other simple models in the literature, this model exhibits, according to the hosts' or pathogen's parameter values, or to the initial infection size, a rich repertoire of behaviours: immediate clearing of the pathogen through aspecific immune response; or acute infection followed by clearing of the pathogen through specific immune response; or uncontrolled infections; or acute infection followed by convergence to a stable state of chronic infection; or periodic solutions with intermittent acute infections. The model can also mimic some features of immune response after vaccination. This model could be a basis on which to build epidemic models including immunological features.

Key words: mathematical model, immune response, pathogen dynamics, vaccination, bifurcations

1 Introduction

Several recent papers [1–3] have started to bring immunological considerations into models for epidemic spread, especially concerning the evolution of virulence [4,5]. Gilchrist and Sasaki [4] have developed the so-called 'nested' approach, in which an explicit model of pathogen-immune response dynamics within each individual host is coupled to a model of epidemic spread between hosts; an approach that has been followed in [5–7]. The idea of integrating host immune response in population models had arisen also in studies of the dynamics of macroparasites [8], especially when the impact of phenomena like waning immunity is investigated.

While an accurate modelling of the dynamics of the interactions between pathogens and the several types of immune cells is a fascinating subject (see for instance [9–11]), in a 'nested' approach the immunological model needs be reasonably simple, but able to qualitatively reproduce the basic behaviour of disease dynamics caused by different pathogen agents.

Models that include different types of immune cells have been used as an ingredient of epidemic models by Kostova [7] and have been fitted to data on CD8 T cell responses in HIV [12] and choriomeningitis [13] infections.

Since we do not aim at an accurate model of immune response, but simply to a phenomenological description of the time course of infections, we follow instead the approach used in [14,4,5] and in several models in [9] of describing the immune response through a single variable, the level of pathogen-specific

* Corresponding author.
Email addresses: pugliese@science.unitn.it (Andrea Pugliese), alberto.gandolfi@iasi.cnr.it (Alberto Gandolfi).
[1] Supported in part by the project EPICO of the Province of Trento, Italy

immunity, that may represent some precise quantity, like the density of specific B-cells or T-cells or antibodies, or a more generic index related to the different types of immune cells specific for that pathogen agent. Analogously, the pathogen load is described through a single variable, giving thus rise to a two-dimensional dynamical system.

Most dynamical description of pathogen-immune interactions give rise to a stereotyped behaviour. Some models [4,5] are tailored for a short-term description of successful immune response: thus, for all parameter values, an infection gives rise to a strong and persistent immunity, that completely clears the pathogen. Other models [14,9] consider long-term effects, such as immunity decay, and share some properties of epidemic models; one may define a number R representing pathogen's reproduction ratio: when $R > 1$, from any initial inoculum a sizeable infection will occur, followed by a growth in immune response reducing the infection to a positive equilibrium, where the pathogen persists at a positive (possibly low) level contrasted by host's immune response; on the other hand, when $R < 1$, the infection cannot start and the immune system eventually completely clears the pathogen.

We build here a slightly more complex model, that considers also the effect of aspecific immune response, such as mediated by macrophages, and Holling-type functional responses of immune cells to pathogen level. We show that this slight increase in complexity allows for a much more diverse behaviour of the system, according to parameter values and initial conditions. Hence, we believe that the resulting may be a satisfactory flexible description of the qualitative features of the dynamical interactions between pathogens and immune system.

2 The model

We describe an infected individual through its pathogen load P and its level of specific immunity B. The variable B may represent some precise quantity, like the density of specific B-cells or antibodies, or a more generic index related to the different types of immune cells specific for that pathogen agent.

As discussed in the Introduction, several authors have described the interactions of a pathogen and its host's immune response through a dynamical system involving these 2 variables. Gilchrist and Sasaki [4] used the following model, where r is the pathogen's replication rate, the immune cells proliferate proportionally (with a proportionality constant a) to the pathogen load, and the pathogen is killed by immune cells with a Lotka-Volterra-type predator-prey relationship with constant c:

$$\begin{cases} P' = rP - cBP \\ \\ B' = aBP \end{cases} \tag{1}$$

The system has to be completed with initial conditions $P(t_0) = P_0 > 0$, $B(t_0) = B_0 > 0$. It is very easy to see (actually system (1) can be transformed, changing t into $-t$, into the classical Kermack-McKendrick epidemic model) that $P(t)$ initially increases (if $r > cB_0$) to a maximum and then declines to 0, while $B(t)$ increases to an asymptotic level (depending on initial conditions) B_∞. Hence, every infection is, after an acute phase, completely cleared.

André and Gandon [5] simplified (1), by assuming that the proliferation rate of immune cells is independent of pathogen load, as long as it is positive [15],

obtaining the system

$$\begin{cases} P' = rP - cBP \\ \\ B' = \beta B \end{cases} \tag{2}$$

The behaviour of $P(t)$ is similar to the previous case, but has the advantage of being expressed through a closed formula, while $B(t)$ grows to infinity, so that the solution can be adequate only for t not too large.

Mohtashemi and Levins [14] considered instead two other features of the immune system, the spontaneous production (at a very low rate) of specific cells, as well as their decay (these aspects were not considered in [4,5] that are limited to acute infections). Moreover, they assumed instead that immune cells are produced by another compartment (constant in size) proportionally to pathogen load. Thus they studied the system

$$\begin{cases} P' = rP - cBP \\ \\ B' = kP - \delta B + h \end{cases} \tag{3}$$

If we take $P(t) \equiv 0$, i.e. we consider an uninfected individual, it is easy to see that $B(t)$ will approach the equilibrium value h/δ, that can then be considered the typical value for uninfected individual. If we consider the dynamics within an individual infected at time t_0, it is then natural to add to (3) the initial conditions $B(t_0) = h/\delta$, $P(t_0) = P_0 > 0$, where P_0 is the inoculum size.

If the threshold condition $r > ch/\delta$ is satisfied, the pathogen-free equilibrium $(0, h/\delta)$ is unstable, and pathogen load will initially increase; then $(P(t), B(t))$ will converge to the positive equilibrium $\left(\frac{\delta r}{c} - h\right)\frac{1}{k}$ which is globally stable [16]. Otherwise, if $r \leq ch/\delta$, the pathogen load immediately starts decreasing

and the infection is completely cleared. In summary, there are only two possible behaviours: either an infection fails immediately, or, if it initially succeeds, it leads to an equilibrium where the pathogen is maintained at low density.

Several other models are proposed in Nowak-May [9] for virus-immune dynamics, but all share this feature: if an infection is possible, it is never cleared completely. It must be remarked that, if the deterministic model is viewed as an approximation of a more realistic stochastic model, it is possible (or perhaps likely) that stochastic extinction of pathogen agents occurs when the pathogen load, as predicted by the deterministic model, is low.

Kostova [7] extends these models, by considering two types of immune cells: effector T cells and memory T cells. Assuming that the latter do not decay at all, the typical behaviour of the system is an acute infection, controlled first by effector T cells, then by memory T cells, until complete clearance of the pathogen.

Here we propose and analyze another extension of model (3), sharing part of the structure with the model proposed by d'Onofrio [17] for tumour–immune interactions, but with the inclusion of aspecific immune response. The resulting model exhibits a rich dynamical repertoire, allowing for acute infection, possibly dose-dependent, followed by deterministic pathogen clearance, or for chronic infection, possibly with periodic fluctuations in pathogen load and immune response. We assume that the predation of immune cells on pathogens follows a Holling function of the 2nd type , and moreover we postulate that a similar action is performed by aspecific cells, whose density is a constant M. Thus, the first equation of (1), (2), or (3) is modified to

$$P' = rP - \frac{c_s P}{1 + a_s P} B - \frac{c_u P}{1 + a_u P} M. \tag{4}$$

As for the second equation, we keep the spontaneous production and the decay of specific immune cells as in (3), but assume, as in (1), auto-replication of specific immune cells, stimulated by pathogen load, but with a maximum replication rate. The resulting equation is

$$B' = \frac{kP}{1 + k_m P} B - \delta B + h. \tag{5}$$

It is convenient to rescale the variables, so as to obtain a non–dimensional system. We choose the following changes of variables:

$$x = \frac{kP}{\delta} \qquad y = \frac{c_s B}{\delta} \qquad \tau = \delta t.$$

Letting $\dot{=}\frac{d}{d\tau}$, we obtain the system

$$\begin{cases} \dot{x} = \alpha x - \dfrac{xy}{1 + \beta_s x} - \dfrac{mx}{1 + \beta_u x} \\ \dot{y} = \qquad \dfrac{xy}{1 + \gamma x} - y + \eta \end{cases} \tag{6}$$

where

$$\alpha = \frac{r}{\delta} \quad \beta_s = \frac{a_s \delta}{k} \quad \beta_u = \frac{a_u \delta}{k} \quad \gamma = \frac{k_m \delta}{k} \quad \eta = \frac{c_s h}{\delta^2} \quad m = \frac{c_u M}{\delta}.$$

Before proceeding with the analysis, we make the following minimal assumptions on the parameters of system (6):

(1) The replication rate of the specific immune cells is higher than their decay rate, at least when the pathogen load is very high. Looking at (5), this translates into $\frac{k}{k_m} > \delta$, i.e. $\gamma < 1$.

(2) The specific immune response responds better to high pathogen loads

than the aspecific response. This translates into $a_s < a_u$, i.e. $\beta_u > \beta_s \geq 0$.

There may be other natural assumptions on the order of magnitude of the parameters, but they are not needed in a preliminary analysis.

3 Equilibria and null-clines

System (6) has clearly the pathogen-free equilibrium $(0, \eta)$.

In order to look for other equilibria, consider the null-clines.

Letting $\dot{y} = 0$, we obtain

$$y = f(x) := \frac{\eta}{1 - \frac{x}{1+\gamma x}}. \tag{7}$$

The function f is positive for $x < x_{imm} = \frac{1}{1-\gamma}$, which is a vertical asymptote. $x_{imm} > 0$, because of Assumption 1. f is increasing and convex in $[0, x_{imm})$.

Letting $\dot{x} = 0$, we obtain

$$y = g(x) := (1 + \beta_s x)\left(\alpha - \frac{m}{1 + \beta_u x}\right). \tag{8}$$

Computing the derivatives, one sees that g is increasing and concave, because of Assumption 2.

Summarizing, the signs of the time derivatives of x and y are as follows:

- $\dot{y} > 0$ for all $x \geq x_{imm}$ and, when $x \in [0, x_{imm})$, $\dot{y} < 0$ for $y > f(x)$.
- $\dot{x} > [<]0$ for $y < [>]g(x)$.

From this information about f and g one obtains (see Fig. 1) the following

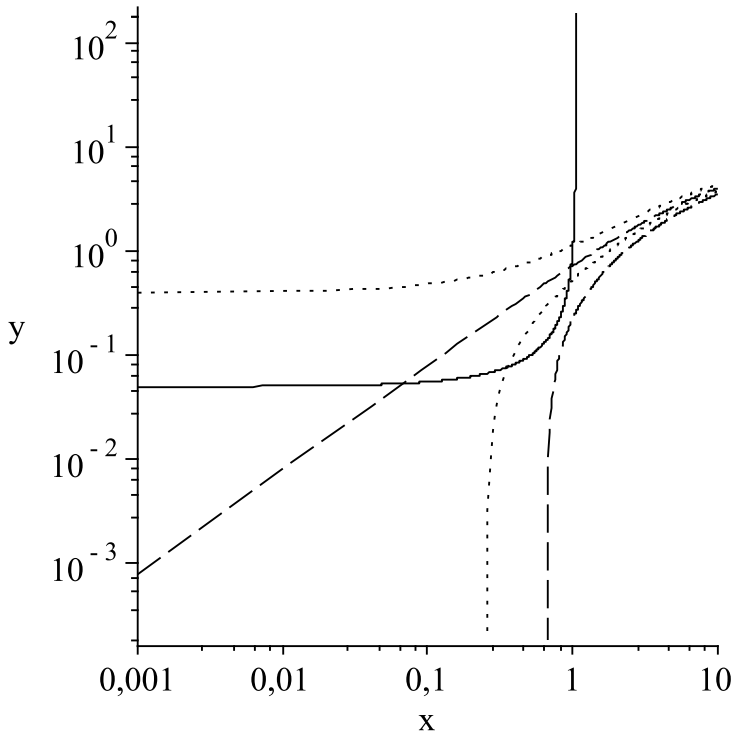

Fig. 1. The function f (solid line) and four instances of the function g (dotted and dashed lines) for different values of $\alpha = 7.5, 7.8, 8, 8.4$. Other parameter values are $\eta = 0.05$, $\gamma = 0.05$, $m = 8$, $\beta_s = 10^{-10}$, $\beta_u = 0.1$.

conclusion:

- if $g(0) > f(0)$, i.e. $\alpha - m > \eta$, there exists a unique $x^* \in (0, x_{imm})$ such that $f(x^*) = g(x^*)$. This corresponds to a positive equilibrium $(x^*, y^* = f(x^*))$ of (6);
- if $g(0) < f(0)$, there may be 0 or 2 solutions (1 in non-generic cases) of $f(x) = g(x)$. Some conditions that guarantee that there are no solutions (hence, no positive equilibria of (6)) are $g'(0) \leq f'(0)$ or $g(x_{imm}) \leq f(0)$.

Recalling the definitions of f and g, and checking also the Jacobian of (6) at the equilibria, one obtains

Proposition 1 • *If $\alpha > \eta + m$, the pathogen-free equilibrium is unstable and there exists a unique positive equilibrium (x^*, y^*). (x^*, y^*) may be lo-*

cally asymptotically stable or unstable; in the latter case, if the solutions are bounded (see Prop. 2 below), Poincaré-Bendixson theory implies the existence of a periodic solution surrounding the equilibrium.

- *If $\alpha < \eta + m$, the pathogen-free equilibrium is locally asymptotically stable, and there exist either 0, 1 and 2 positive equilibria. If there are 2 positive equilibria (x_1^*, y_1^*) and (x^*, y^*) with $x_1^* < x^*$, then (x_1^*, y_1^*) is a saddle point, while (x^*, y^*) may be asymptotically stable or unstable; in the latter case, it may be an unstable focus, or an unstable node.*

Proof. Most statements follow immediately from the above arguments. We need only to check the Jacobian of (6) at a positive equilibrium (x^*, y^*). Through some computations, we obtain

$$J^* = \begin{pmatrix} \alpha - \frac{y^*}{(1+\beta_s x^*)^2} - \frac{m}{(1+\beta_u x^*)^2} & -\frac{x^*}{1+\beta_s x^*} \\ \frac{y^*}{(1+\gamma x^*)^2} & \frac{x^*}{1+\gamma x^*} - 1 \end{pmatrix}$$

$$= \begin{pmatrix} \frac{x^*}{1+\beta_s x^*} g'(x^*) & -\frac{x^*}{1+\beta_s x^*} \\ \eta \frac{f'(x^*)}{f(x^*)} & -\frac{\eta}{f(x^*)} \end{pmatrix} \quad (9)$$

It follows

$$\det(J^*) = \frac{x^*}{1+\beta_s x^*} \frac{\eta}{f(x^*)} (f'(x^*) - g'(x^*)). \quad (10)$$

If there is only 1 equilibrium, we have (generically) $f'(x^*) > g'(x^*)$ (see Fig. 1); if there are 2 equilibria, we have $f'(x_1^*) < g'(x_1^*)$ and $f'(x^*) > g'(x^*)$. We then have from (10) that (x_1^*, y_1^*) has 2 eigenvalues of opposite sign, so that it is a saddle point; on the other hand, to ascertain the stability of (x^*, y^*) , we need to study the sign of $\mathrm{tr}(J^*) = \frac{x^*}{1+\beta_s x^*} g'(x^*) - \frac{\eta}{f(x^*)}$, which may be either positive or negative. □

The different possibilities are outlined in Fig. 3 and 4, where the phase plane and some typical solutions are plotted for different values of the parameter α.

Since the parameters α and $\eta+m$ represent the replication rate of the pathogen and, respectively, the overall efficacy of the immune system (see Eq. (4)), we note that the condition $\alpha > \eta+m$ corresponds to a case of very high virulence capable of overcoming the non-specific immunity, whatever the extent of the initial infection.

From the phase plane, one may note that in principle there may exist solutions diverging to $+\infty$ with both $x(t)$ and $y(t)$ increasing, and with $y(t) < g(x(t))$. In the Appendix, we show the following

Proposition 2 *If $\beta_s = 0$ or $\gamma = 0$ or $\alpha < \frac{1}{\gamma} - 1$, all solution of (6) starting from (x_0, η) with $x_0 > 0$ are bounded and converge either to an equilibrium or a periodic solution of (6).*

If $\beta_s > 0$ and $\alpha > \frac{1}{\gamma} - 1$, there exist solutions of (6) starting from (x_0, η) with $x_0 > 0$ such that $x(t)$ and $y(t)$ are monotonically increasing and $\lim_{t\to\infty} x(t) = \lim_{t\to\infty} y(t) = +\infty$.

Remark 1 *It is clear from the structure of (6) that diverging solutions are possible, because it is assumed that pathogens grow exponentially, in absence of specific immune response, and that growth may be faster than the maximal growth of immune response. One could change the assumption of pathogen exponential growth, since pathogen growth will eventually be limited by the total host resources. We instead retain the assumption of exponential growth, interpreting diverging solutions as instances in which host defenses are not able to respond to pathogen replication, and infection ends with host death.*

Moreover, we recall that the parameter $1/\gamma$ represents the maximal replication rate of the immune system. Thus is clear and intuitive the meaning of the condition $\alpha > 1/\gamma - 1$, which implies that for sufficiently high initial infections (of a naive individual, i.e. at the basal level of specific immunity) the infection evolves unbounded. Models satisfying this conditions appear to be the most realistic.

Note that β_s or $\gamma = 0$ imply instead that the immune system can always control the infection whatever the initial infection be. Therefore, the Holling type functional form of the pathogen removal *and* of the response of the immune system to pathogen level is, in this model, necessary for the possibility that large infections escape immune control.

4 Bifurcation diagrams and examples

The qualitative behaviour of solutions may be summarized as a bifurcation diagram, choosing as parameter, for instance, α (see Fig. 2). At $\alpha = \alpha_0 := \eta + m$, the equilibrium $(0, \eta)$ undergoes a transcritical bifurcation, which, under the condition $m\beta_u + \eta\beta_s > \eta$, is subcritical, meaning that a positive equilibrium exists unstable for $\alpha < \alpha_0$, α close to α_0. In this case, there will exists $\alpha_1 < \alpha_0$ in which the positive equilibrium undergoes a saddle-node bifurcation.

For $\alpha < \alpha_1$ there are no positive equilibria, and the pathogen–free equilibrium $(0, \eta)$ is asymptotically stable; actually, if all solutions are bounded (Prop. 2), Poincaré-Bendixson theory implies that it is globally attractive from positive initial points. Still, the system is excitable, in the sense that if the initial pathogen dose x_0 is sufficiently large, then, starting from (x_0, η), $x(t)$ grows to high values before the solution eventually approaches $(0, \eta)$.

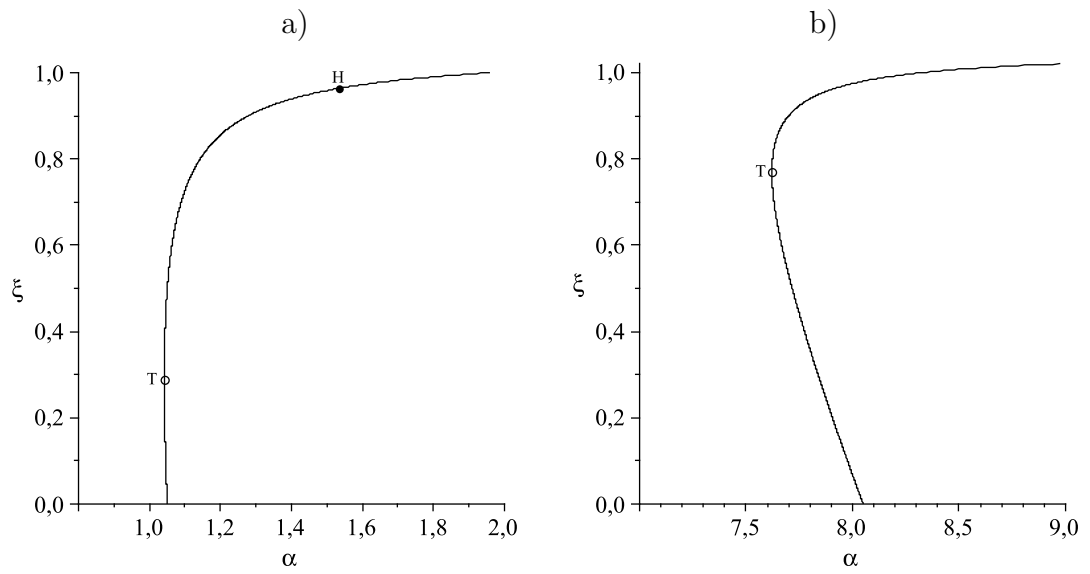

Fig. 2. The bifurcation diagram of equilibria with respect to α. The circle with H corresponds to the value (at $\alpha = \alpha_H$) of Hopf bifurcation; the circle with T to the tangent (saddle-node) bifurcation at $\alpha = \alpha_1$. Parameter values are $\eta = 0.05$, $\gamma = 0.05$, $\beta_s = 10^{-10}$, $\beta_u = 0.1$. In the left panel a), $m = 1$; in the right panel b) $m = 8$.

For $\alpha_1 < \alpha < \alpha_0$, the pathogen–free equilibrium $(0, \eta)$ is still asymptotically stable, but there also two positive equilibria (x_1^*, y_1^*) and (x^*, y^*) with $x_1^* < x^*$. For $\alpha > \alpha_0$, there exists a unique positive equilibrium (x^*, y^*), and no solution with $x_0 > 0$ will approach the pathogen-free equilibrium.

Concerning the stability of the positive equilibria, we can say that, when there are two equilibria ($\alpha_1 < \alpha < \alpha_0$), the lower one (x_1^*, y_1^*) is an unstable saddle point. Moreover, when α is large enough, the equilibrium (x^*, y^*) is always unstable.

There are two possible paths to instability: in one case (see Fig. 2a), (x^*, y^*) is asymptotically stable for α close to (and larger than) α_1; there exists then a value α_H at which the positive equilibrium (x^*, y^*) undergoes a Hopf bifurcation: for $\alpha < \alpha_H$, (x^*, y^*) is asymptotically stable, while it is unstable for $\alpha > \alpha_H$. In Fig. 3, we show the phase plane of solutions for $\alpha < \alpha_H$ and for

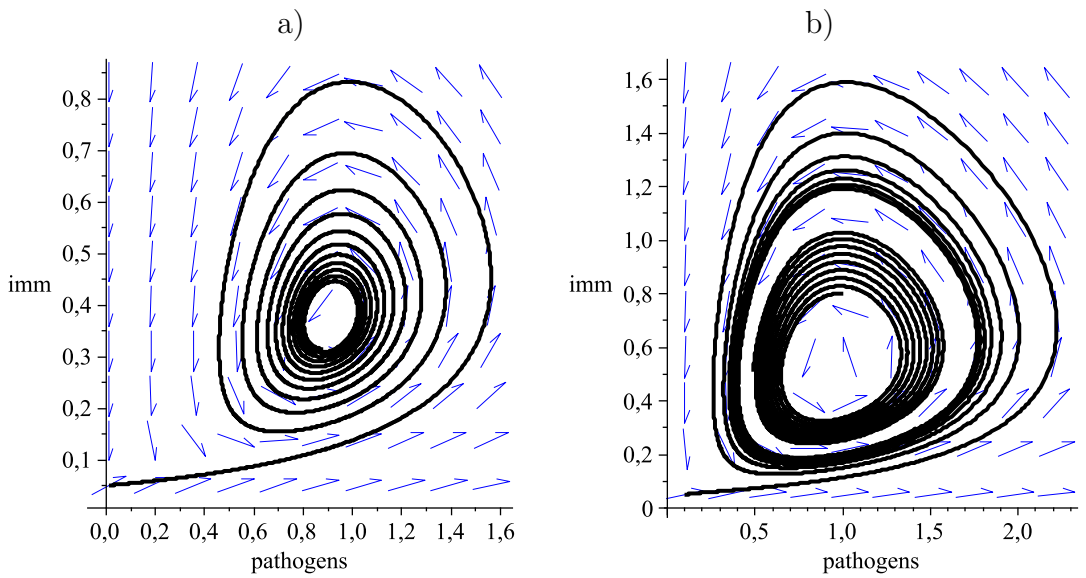

Fig. 3. Examples of the phase plane of the system (6). Parameter values are $\eta = 0.05$, $\gamma = 0.05$, $\beta_s = 10^{-10}$, $\beta_u = 0.1$, $m = 1.5$. In the left panel a), $\alpha = 1.75$; the solution shown is slowly converging to the equilibrium at the centre of the spiral. in the right panel b) $\alpha = 1.9$; two solutions are shown, one starting from $(0.1, \eta)$ and spiraling inwards, the other one starting from $(1, 0.8)$ and spiraling outwards; both are converging to a limit cycle in between.

$\alpha > \alpha_H$. It may also happen that there are several Hopf bifurcation values, with the positive equilibrium alternately losing and acquiring stability.

In the other case (Fig. 2b), the equilibrium (x^*, y^*) is unstable for all α. The limit cycle existing for $\alpha > \alpha_0$ because of Poincaré-Bendixson theory, emerges through a homoclinic bifurcation at $\alpha = \alpha_0$. Numerically, it appears that, for $\alpha < \alpha_0$, all solutions (except for the exceptional ones lying on the stable manifold of (x_1^*, y_1^*)) converge to $(\eta, 0)$, while for $\alpha > \alpha_0$ they converge to a periodic solution (see Fig. 4).

There exists moreover a value $\alpha_\infty = \frac{1}{\gamma} - 1$, such that for $\alpha < \alpha_\infty$ all solutions are bounded, and converge to one of the previous alternatives; for $\alpha > \alpha_\infty$, there exist diverging solutions of (6).

Under the condition $m\beta_u + \eta\beta_s < \eta$ (which seems less likely, since entails a large

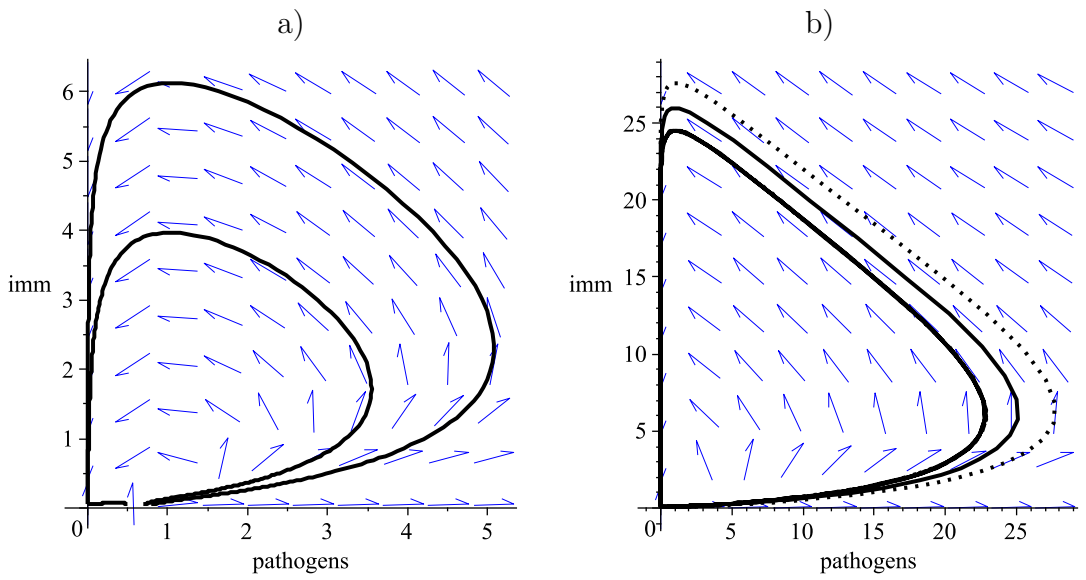

Fig. 4. Examples of the phase plane of the system (6). Parameter values are $\eta = 0.05$, $\gamma = 0.05$, $\beta_s = 10^{-10}$, $\beta_u = 0.1$, $m = 8$. In the left panel a), $\alpha = 7.6215$; three solutions are shown: the left one starting from $(0.5, 0.05)$ converges to $(0, \eta)$ with a monotone decrease of $x(t)$, while $y(t)$ remains very close to η; the two other solutions, starting from $(0.7, \eta)$ and $(0.8, \eta)$ converge to $(0, \eta)$ after an initial increase (rather different between them) of $x(t)$. in the right panel b) $\alpha = 8.5$; two solutions are shown, one (dotted line) starting from $(0.8, \eta)$, the other one (solid line) starting from $(0.5, \eta)$: both appear to converge to a limit cycle (basically what appears to be the middle curve) which, for a part, lies very close to the y-axis.

spontaneous production of effective immune cells), the bifurcation diagram is simpler with a supercritical bifurcation of the pathogen–free equilibrium at α_0 and a unique positive equilibrium for $\alpha > \alpha_0$.

5 Examples of behaviour of the model

First of all, we show how different behaviours of the system may occur by changing the inoculum size or parameters of the model, reflecting individual variation.

In Fig. 5 we show some examples of the time course of infections.

The solid lines correspond to three different initial sizes of the inoculum: it

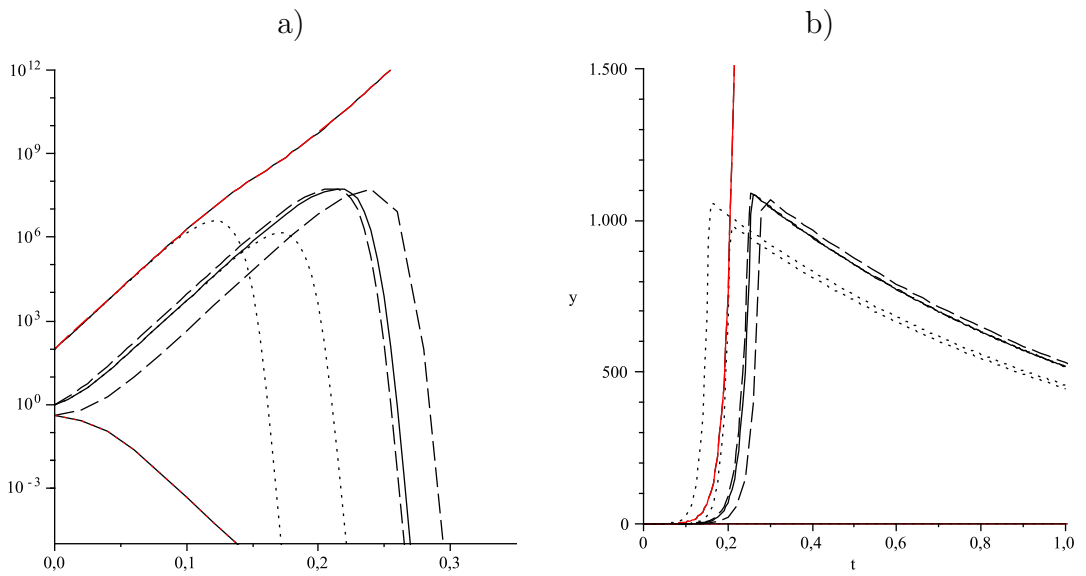

Fig. 5. Examples of the time course of solutions of the system (6). In the left panel a), pathogen load $x(t)$ in logarithmic scale; in the right panel b), immunity level $y(t)$. The solid lines are obtained, for different initial conditions $(0.4, \eta)$, $(1, \eta)$ and $(100, \eta)$, with parameter values $\eta = 0.05$, $\gamma = 0.02$, $\beta_s = 10^{-8}$, $\beta_u = 2$, $m = 200$, $\alpha = 100$. The dotted lines are obtained, from the same initial conditions, with $\beta_u = 1.5$, $\gamma = 0.015$, $\beta_s = 7.5 \cdot 10^{-9}$; the one starting from $(0.4, \eta)$ is identical to (and hidden from) the solid line. The dashed lines are obtained, from the same initial conditions, with $m = 150$; the one starting form $(100, \eta)$ is identical to (and hidden from) the solid line.

can be seen that, all other things beings the same, this may lead to a sub-threshold infection, or to a normal infection later controlled by immunity, or to a catastrophic infection corresponding, from the mathematical point of view, to a diverging solution, and, from the biological point of view, to a potentially lethal event.

The dotted lines corresponds to the same initial inocula in an individual whose immune cells replicate faster; this corresponds to a higher k in terms of the original parameters, hence smaller β_s, β_u and γ for adimensional parameters. In this case, the infection is always controlled.

The dashed lines simulate the same initial inocula in an individual with a lower level of aspecific response (M); now also the smaller inoculum size leads to a

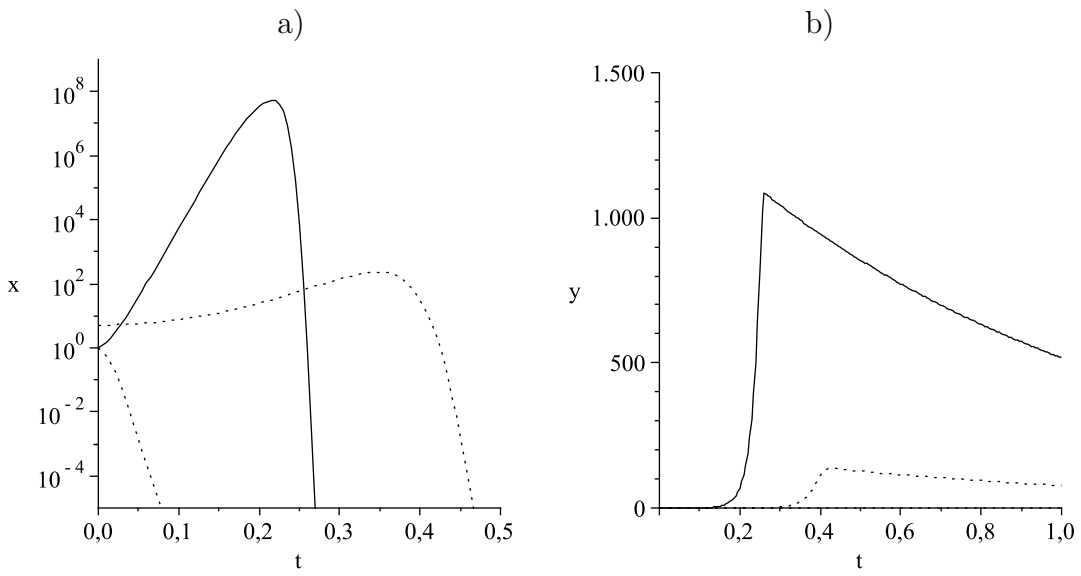

Fig. 6. Simulation of vaccination with system (6). In the left panel a), pathogen load $x(t)$ in logarithmic scale; in the right panel b), immunity level $y(t)$. The solid line is obtained with initial condition $(1, \eta)$ and parameter values $\eta = 0.05$, $\gamma = 0.02$, $\beta_s = 10^{-8}$, $\beta_u = 2$, $m = 200$, $\alpha = 100$. The dotted lines simulate vaccination and are obtained with $\alpha = 20$ and initial conditions $(1, \eta)$ and $(5, \eta)$.

normal infection, while, in the other cases, the simulations are very similar to the reference ones (solid lines).

We then consider what could be the effect of vaccination, modelled in an extremely simple way. We assume that vaccination is realized by inoculating an attenuated pathogen in the sense that its replication rate α is lower than the wild type; in all other respects, the attenuated pathogen is identical to the wild-type, so that the immune response is the same.

In Fig. 6, we compare the time courses of a normal infection with that of a vaccination. In the example, when the vaccine inoculum is too small (in the Figure, a same size inoculum of the wild type leads to an infection), the pathogen content decreases immediately and no effective immune response mounts. With a larger inoculum, one obtains an attenuated infection (the peak value of $x(t)$ is several orders of magnitude smaller than in a normal in-

fection) and an immune response that, while lower than in the case of a normal infection, is still protective. Thus the model can reproduce both vaccination failures (the threshold for the initial inoculum depends on the other parameters m, β_u, ... that may be different among individuals), and the protective effect of vaccination.

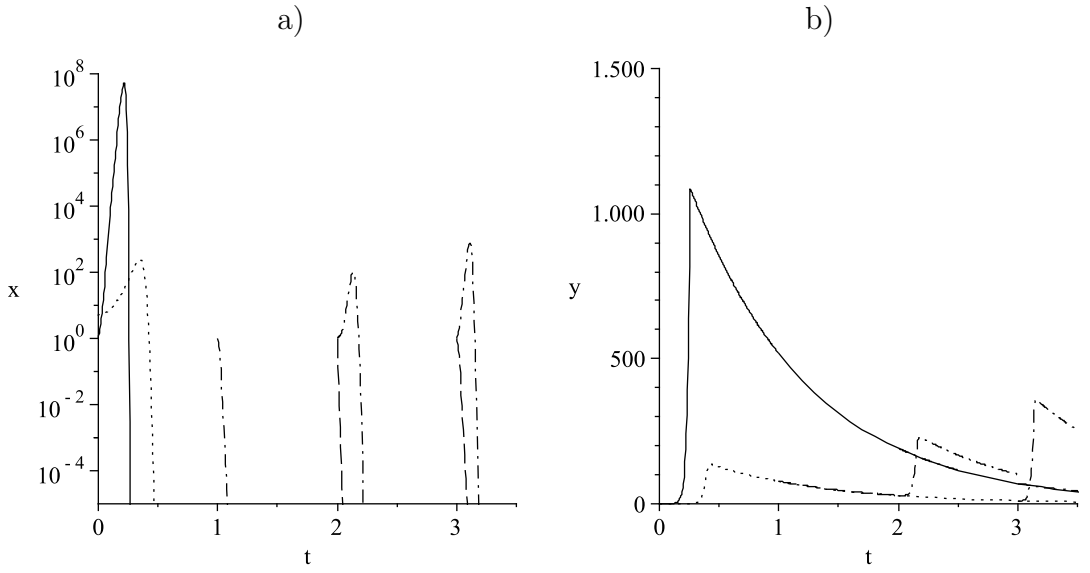

Fig. 7. Reinfections in naturally infected and vaccinated individuals. In the left panel a), pathogen load $x(t)$ in logarithmic scale; in the right panel b), immunity level $y(t)$. The solid line corresponds to a natural infection and is the same as in Fig. 6. The dotted line corresponds to a vaccinated individual and is the same as in Fig. 6 with initial condition $(5, \eta)$. The dashed lines correspond to reinfections (at $t = 1,\ 2$ or 3) of the naturally infected individual (these cannot be seen in panel b), since almost no change occurs in immunity level). The dot-and-dash lines correspond to reinfections (at $t = 1,\ 2$ or 3) of the vaccinated individual. In the reinfections $\alpha = 100$, like in the natural infection.

The protective effect can be seen in Fig. 7. There we show the results of some simulations in which after an initial vaccination or normal infection, the individual is reinfected, at fixed times after the initial infection, with the normal pathogen. It can be seen that when the second infection occurs not too long after the first one (in the Figure at $t = 1$), whether it is vaccination or natural infection, the new infection is immediately cleared and the immunity is not boosted. Waiting a longer time for the second infection ($t = 2$ or $t = 3$), still

there are no effects in the case of a naturally infected individuals; however, after a vaccination, a mild infection occurs (similar to that occurring immediately after vaccination) with a boosting of the immune response; in this case, immunity level actually becomes higher than in the case of a naturally immunized individual. If the second infection occurs long after initial vaccination (not shown in the figures), without any exposure to the pathogen in the mean time, then immunity has dropped so low that the new infection is similar to that occurring in a naive individual. A similar reinfection in a naturally infected individual would instead lead to mild infection, and a boosting of the infection.

It seems that this simple model is able to mimic several of the phenomena occurring in vaccinations, from failures, to waning immunity with time, and boosting of immunity through reexposures at the correct schedules. It may also occur that while moderate reexposures lead to very mild reinfections and boosting of immunity, extreme reexposures lead to significant reinfections, as documented for measles [18]. Models of this type could then be useful for an appropriate design of revaccination schedules, that would depend on how much the pathogen is circulating in the population. In fact, the model, at least for the parameter values used in this simulation, predicts that an effective immunity can be maintained as long as an individual is confronted, from time to time, with the pathogen. As natural exposures become rare, then revaccinations need be more frequent.

There is a long-standing debate on the mechanisms maintaining immunity in individuals, whether it is due to very long-lived memory cells, or residual antigenic stimulation [19,20]. Varying the parameter values, this model can support any of these. In terms of the original parameters, $1/\delta$ is the average

duration of a B-particle; if this time is of the order of magnitude of human life, then no other mechanisms are needed. On the other hand, with a larger δ, maintenance of immunity is compatible either with convergence of the system to a stable positive equilibrium (phenomenon that seems to be possible only when α is moderately large, i.e. with slowly replicating pathogens) or with not too infrequent reexposures to the pathogen.

References

[1] J. Dushoff, Incorporating immunological ideas in epidemiological models, J. theor. Biol. 180 (1996) 181–187.

[2] B. Hellriegel, Immunoepidemiology – bridging the gap between immunology and epidemiology, Trends Parasitol. 17 (2001) 102.

[3] M. Martcheva, S. Pilyugin, An epidemic model structured by host immunity, J. Biol. Systems 14 (2006) 185–203.

[4] M. Gilchrist, A. Sasaki, Modeling host-parasite coevolution, J. theor. Biol. 218 (2002) 289–308.

[5] J.-B. André, S. Gandon, Vaccination, within-host dynamics, and virulence evolution, Evolution 60 (2006) 13–23.

[6] M. Gilchrist, D. Coombs, Evolution of virulence: interdependence, constraints and selection using nested models, Theor. Pop. Biol. 69 (2006) 145–153.

[7] T. Kostova, Persistence of viral infections on the population level explained by an immunoepidemiological model, Math. Biosci. 206 (2007) 309–319.

[8] M. Woolhouse, A theoretical framework for the immunoepidemiology of helminth infection, Parasite Immunology 14 (1992) 563–578.

[9] M. A. Nowak, R. May, Virus dynamics: Mathematical principles of immunology and virology, Oxford Univ. Press, 2000.

[10] A. Perelson, Modeling viral and immune system dynamics, Nature Rev. 2 (2001) 28.

[11] D. Wodarz, Killer Cell Dynamics. Mathematical and Computational Approaches to Immunology, Springer, 2007.

[12] V. Müller, A. F. M. Marée, R. J. de Boer, Small variations in multiple parameters account for wide variations in HIV-1 set-points: a novel modelling approach, Proc. R. Soc. Lond. B 268 (2001) 235–242.

[13] C. L. Althaus, V. V. Ganusov, R. J. de Boer, Dynamics of CD8 T cell responses during acute and chronic lymphocytic choriomeningitis virus infection, The Journal of Immunology 179 (2007) 2944—2951.

[14] M. Mohtashemi, R. Levins, Transient dynamics and early diagnosis in infectious disease, J. Math. Biol. 43 (2001) 446–470.

[15] R. Antia, C. T. Bergstrom, S. S. Pilyugin, S. M. Kaech, R. Ahmed., Models of $CD8^+$ responses. 1. What is the antigen-independent proliferation program?, J. Theor. Biol. 221 (2003) 585–598.

[16] A. Whitman, H. Ashrafiuon, Asymptotic theory of an infectious disease model, J. Math. Biol. 53 (2006) 287–304.

[17] A. d'Onofrio, A general framework for modeling tumor-immune system competition and immunotherapy: Mathematical analysis and biomedical inferences, Physica D 208 (2005) 220–235.

[18] M. Paunio, H. Peltola, O. P. Heinonen, Explosive school-based measles outbreak: Intense exposure may have resulted in high risk, even among revaccinees., American J. Epidem. 148 (1998) 1103.

[19] D. Gray, Immunological memory, Annu. Rev. Immunol. 11 (1993) 49–77.

[20] T. Kundig, M. Bachmann, P. Ohashi, H. Pircher, H. Hengartner, R. Zinkernagel, On T cell memory: arguments for antigen dependence, Immunol. Rev. 150 (1996) 63–90.

A Boundedness of solutions

We prove here Proposition 2.

Let us prove the boundedness of trajectories when $\alpha < \frac{1}{\gamma} - 1$ [or $\gamma = 0$ or $\beta_s = 0$]; we show that for each $x_0 > 0$, the solution of (6) starting from (x_0, η) is trapped in a bounded invariant set; hence the conclusion follows.

Choose δ such $\alpha < \frac{1}{\gamma} - 1 - \delta$ and take $M \geq \max\{x_0, \ \frac{\frac{1}{\gamma} - \delta}{\gamma\delta}\}$ and such that $g(M) > \eta$. Hence, for each $x \geq M$

$$\frac{x}{1+\gamma x} \geq \frac{1}{\gamma} - \delta \quad \text{and} \quad g(x) > 0. \tag{A.1}$$

Take the solution of (6) starting from (M, η) and assume that it remains for all $t > 0$ in the set $\{y < g(x)\}$. We would then have $\dot{x} > 0$ and $\dot{y} > 0$ for all $t > 0$, and we could write $y(t) = h(x(t))$ for an increasing function h.

Then

$$h'(x) = \frac{h(x)\left(\frac{x}{1+\gamma x} - 1\right) + \eta}{x\left(\alpha - \frac{h(x)}{1+\beta_s x} - \frac{m}{1+\beta_u x}\right)} \geq \frac{h(x)\left(\frac{1}{\gamma} - \delta - 1\right)}{\alpha x} \tag{A.2}$$

using (A.1). By a comparison principle, we obtain

$$h(x) \geq \eta \left(\frac{x}{M}\right)^{\frac{\frac{1}{\gamma} - \delta - 1}{\alpha}} \quad \forall\ x \geq M. \tag{A.3}$$

Since, if $\beta_s > 0$, $g(x)$ grows linearly, while $h(x)$ grows superlinearly, necessarily

there must exist $x_M > x$ such that $h(x_M) = g(x_M)$ and $h(x) < g(x)$ for $M < x < x_M$. This means that the solution of (6) starting from (x_0, η) enters the region $\{y > g(x)\}$ where $\dot{x} < 0$. This will be the first part of the boundary of the invariant region.

If $\beta_s = 0$, one needs only choose δ such that $\frac{1}{\gamma} - 1 - \delta > 0$; the same argument would then show that $h(x)$ grows with a positive exponent, while $g(x)$ tends to a constant, again proving the existence of $x_M > x$ such that $h(x_M) = g(x_M)$.

Finally, if $\gamma = 0$, one has to choose $M \geq \max\{x_0, \alpha + 1 + \delta\}$ with $\delta > 0$ and repeat the same argument.

Consider now the solution of (6) starting from $(x_M, y_M = g(x_M))$ for any $x_M > \frac{1}{1-\gamma}$. Initially we have $\dot{x} < 0$ and $\dot{y} > 0$, but we prove that eventually the trajectory enters the region $C = \{x < \frac{1}{1-\gamma}, y > f(x)\}$ where $\dot{y} < 0$.

Assume the opposite. Then, since $y(t)$ is monotone increasing, and no equilibria exist with $y > y_M$, necessarily we have $\lim_{t \to \tau^-} y(t) = +\infty$, where $[0, \tau)$ is the maximal interval of existence of solutions. Since $x(t)$ is monotone decreasing, we have $\lim_{t \to \tau^-} x(t) = x_m$. Since we have assumed that $(x(t), y(t))$ never enters the region C, necessarily (see Fig. 1) we have $x_m \geq \frac{1}{1-\gamma}$.

First of all, we show that $\tau = +\infty$. In fact, if $\gamma > 0$, we have $\dot{y} \leq \left(\frac{1}{\gamma} - 1\right) y$; this implies an exponential bound for $y(t)$, thus global existence. If $\gamma = 0$, we have $\dot{x} \leq \alpha x - \frac{xy}{1+\beta_s x_M}$ so that

$$\frac{d}{dt}\left((1 + \beta_s x_M)x(t) + y(t)\right) \leq \alpha(1 + \beta_s x_M)x(t) - y(t) + \eta$$

$$\leq \alpha\left((1 + \beta_s x_M)x(t) + y(t)\right) + \eta$$

which again yields an exponential bound for $((1 + \beta_s x_M)x(t) + y(t))$, thus

global existence.

Now, let T be such that $y(T) > K$ with $K \geq y_M$ to be chosen later. From (6), we then obtain, for $t > T$,

$$\dot{x} \leq \alpha x - \frac{K}{1-\gamma+\beta_s} - \frac{m}{1-\gamma+\beta_u}.$$

The comparison principle then implies

$$x(t) \leq e^{\alpha t}\left(x_M - \left(\frac{K}{1-\gamma+\beta_s} + \frac{m}{1-\gamma+\beta_u}\right)\frac{1}{\alpha}\right) + \left(\frac{K}{1-\gamma+\beta_s} + \frac{m}{1-\gamma+\beta_u}\right)\frac{1}{\alpha}. \tag{A.4}$$

If K has been chosen large enough that the coefficient of $e^{\alpha t}$ in (A.4) is negative, we have $\lim_{t\to\infty} x(t) = -\infty$, reaching a contradiction.

There exists then a point (x_C, y_C) with $x_C < \frac{1}{1-\gamma}$ and $y_C = f(x_C)$ where the trajectory enters the region C.

The boundaries of the bounded invariant set $\mathcal{B}$ are then the two arcs of trajectory from (M, η) to $(x_M, g(x_M))$, and then from $(x_M, g(x_M))$ to $(x_C, f(x_C))$, and the segments $\{(x, f(x_C)),\ x \in [0, x_C]\}$, $\{(0, y),\ y \in [\eta, f(x_C)]\}$, $\{(x, \eta),\ x \in [0, M]\}$.

The solution of (6) starting from (x_0, η) [where $x_0 > 0$ is arbitrary] remains inside $\mathcal{B}$, hence is bounded.

Assume now $\alpha > \frac{1}{\gamma} - 1$ and $\beta_s > 0$. Take the solution of (6) starting from (x_0, η) with $x_0 > 0$ to be chosen later. From the second of (6), we obtain

$$y(t) \leq \frac{\eta}{1-\gamma} e^{\left(\frac{1}{\gamma}-1\right)t}. \tag{A.5}$$

Then we have

$$\dot{x} \geq \alpha x - \frac{\eta}{\beta_s(1-\gamma)} e^{\left(\frac{1}{\gamma}-1\right)t} - \frac{m}{\beta_u}. \tag{A.6}$$

which implies

$$x(t) \geq \left(x_0 - \frac{\eta}{(1-\gamma)\beta_s\left(\alpha - \frac{1}{\gamma} + 1\right)} - \frac{m}{\alpha\beta_u} \right) e^{\alpha t}. \tag{A.7}$$

If x_0 is chosen large enough that the coefficient of $e^{\alpha t}$ in (A.7) is positive, (A.5) and (A.7) together imply

$$y(t) \leq \frac{\eta}{1-\gamma} \left(\frac{x(t)}{x_0 - \frac{\eta}{(1-\gamma)\beta_s\left(\alpha-\frac{1}{\gamma}+1\right)} - \frac{m}{\alpha\beta_u}} \right)^{\frac{\frac{1}{\gamma}-1}{\alpha}}. \tag{A.8}$$

Since $\frac{1}{\gamma} - 1 < \alpha$ and $\beta_s > 0$, this inequality implies, for x_0 large enough, $y(t) < g(x(t))$ so that we obtain a solution lying at all times in the set $\{y < g(x)\}$ so that $\dot{x} > 0$ and $\dot{y} > 0$. Furthermore, the inequality $\dot{x} \leq \alpha x$ implies global existence, and consequently from (A.7) $x(t) \to +\infty$ and

$$\lim_{t\to\infty} x(t) - \lim_{t\to\infty} y(t) = +\infty.$$